Propulsion and Power Research 2012;1(1):12–28

http://ppr.buaa.edu.cn/

Propulsion and Power Research

www.sciencedirect.com

ORIGINAL ARTICLE

# Unsteady cooperative flow in compression system

**Sheng Zhou, Yajun Lu, Anping Hou, Wei Yuan, Zhiping Li***

*National Key Laboratory of Science and Technology on Aero-Engine Aero-Thermodynamics, School of Energy and Power Engineering, Beihang University, Beijing 100191, China*

Received 14 February 2012; accepted 5 November 2012
Available online 20 December 2012

**KEYWORDS**

Unsteady cooperative flow;
Unsteady natural flow;
Time-space structure of the flow field;
Compression system;
Aero-engine;
Flow over multi-bodies;
Asymmetric flow;
Axial compressor transonic flow

**Abstract** When there are several bodies with relative motion in a flow field, such as the flow in the compression system of modern aero-engine, the flow field will have certain special features, one of which is that the time-space structure of such multi-bodies unsteady vorticity flow field would be either of unsteady natural flow (UNF) pattern or of unsteady cooperative flow (UCF) pattern. If we further examine the aerodynamic design system of aero-engine, there is no mechanism for the unsteady cooperative flow to occur, in other words the flow field must be of the unsteady natural flow type. If certain technical measures can be adopted to transform UNF into UCF, the aerodynamic performances will surely be improved. This is the main task the author and their colleague have been devoted to and the results are reviewed in the present paper with emphases laid on basic ideas, technical approaches and experimental verifications.


## 1. Introduction

Around the beginning of new centuries, the group of "Aerodynamic Design of Compression System Layout" of the National Key Laboratory of Science and Technology on Aero-Engine Aero-Thermodynamics began to undertake series of key projects of basic research, focusing on a question: Is there any new mechanism and new approach for the aerodynamic performances of aero-engine compression system to be further improved? After analyzing the basic simplification assumption underlying the modern

*Corresponding author.
E-mail address: leezip@buaa.edu.cn (Zhiping Li)
Peer review under responsibility of National Laboratory for Aeronautics and Astronautics, China.

Production and hosting by Elsevier

2212-540X 
http://dx.doi.org/10.1016/j.jppr.2012.11.001

## Nomenclature

| | |
|---|---|
| $f_e$ | excitation frequency |
| $f_{shed}$ | vortex shedding frequency |
| $\overline{f}_e$ | relative excitation frequency, $\overline{f}_e = f_e/f_{shed}$ |
| $i$ | angle of attack |
| $\dot{m}$ | mass flow |
| $n$ | rotate speed |
| $\overline{n}$ | correct rotate speed |
| $P^*$ | total pressure |
| $Q$ | volume flux |
| $SM$ | stall margin |
| $\tau_{RF}$ | reverse flow time ratio |
| $\pi$ | pressure ratio |
| $\eta$ | efficiency |
| $\sigma$ | total pressure recovery coefficient |
| $\delta$ | coefficient of the relative increment |
| $\Delta$ | coefficient of the absolute increment |

*Superscript and subscript*

| | |
|---|---|
| D | parameters under design condition |
| S | parameters under stall condition |
| cor | correct parameters |
| max | parameters under maximum loading condition |

*Abbreviations*

| | |
|---|---|
| CS | compression system |
| CT | casing treatment |
| UNF | unsteady national flow |
| UCF | unsteady cooperative flow |
| TE | turbine engine |
| WIE | wake impact effects |
| WS | turbofan engine |

aerodynamic design system, we propose a new concept, i.e. “the Unsteady Cooperative Flow in Compression System” (shortened to UCF in CS) [1]. Up to now 14 doctor dissertations have been completed focused on this new idea, in which 2 were awarded the first prize of science and technology by French SAFRAN Group, one evaluated as the 2008 national outstanding doctor dissertation. Since there are numerous projects, equipment, staff members and software related to UCF in CS, these projects lasted dozen years and many graduate students were graduated, it is thought necessary to arrange and publish a review paper to highlight the related academic ideas to guide subsequent graduate students and to solicit valuable opinions from specialists in the same occupation.

For concise and clear presentation, the present paper attempt to lay emphases on physical essence of the new idea, rather than enumerate symbols and formula. Experimental facilities, testing system and computational fluid dynamics (shortened to CFD) software related will not be expounded. Although our experiments and CFD simulations have experienced success and setbacks, only part of them is included to illustrate status quo, and thus the paper consists of five parts:

(1) Introduction.
(2) Idea of UCF in CS.
(3) Technical exploration and arrangements to improve the time–space structure of unsteady vortex flow and the corresponding aerodynamic parameters.
(4) Part of our experiment results to illustrate in Section 4.
(5) Summary in Section 5.

## 2. Unsteady cooperative flow in compressor

When there are several bodies with relative motion in a flow field, such as the flow in the compression system of modern aero-engine, the flow field has certain special features, one of which is that the time–space structure of such multi-bodies unsteady vortex flow field would be either the unsteady natural flow (shortened to UNF) or the unsteady cooperative flow (shortened to UCF). If certain technical measures can be adopted to transform UNF into UCF, the random time–space structures would be transformed into an orderly one. However this character has not been considered in the current aerodynamic design system of aero-engine, and thus there exists a possibility to improve the time-averaged aerodynamic performances by means of transforming the random time–space structure into an orderly one, which will be expounded in the present part.

### 2.1. The compression system’s function and the unsteady vorticity flow

It is well-known that the basic function of the compression system is to boost the incoming flow by doing work on it. The classic Euler formula describes the two elements in the process the rotor blade row does work on the incoming flow, i.e. the circumferential velocity of the rotor blade and the change in the circumferential velocity component of the incoming flow. Unsteady effects in the above-mentioned process was analyzed in the classic literature [2], however, the mechanism of work-doing was not connected to the time–space structure of the unsteady flow field, and thus questions would be asked as follows. (1) What is the role the unsteady flow field plays in the work-doing process? (2) What is the relationship between the unavoidable dynamic energy losses of the flow occurring in the process with the time–space structure of the unsteady flow field? (3) What is the effect the stagger arrangement of the stator blades and the rotor blades has on the time–space structure of the unsteady flow field? (4) There are numerous geometric and aerodynamic parameters in an actual compression system, how should their influences on the time–space structure of the unsteady flow field be considered in the aerodynamic arrangement design of the compression system?

For illustrating the relationship between the unsteady flow field and the work-doing process, we would like to quote directly the famous scientist Professor Lu Shijia's words "essence of the fluid lies in the fact that it cannot endure the action of "shearing", once experienced a shearing, there occur vortexes." As for the compression system, the rotor blade rows exert strong shearing on the incoming flow via rotation, and thus the whole flow field experiences a sharp change, and the essence of the change is the occurrence of an unsteady vorticity field, the characteristics of which will surely affect the compression system's aerodynamic performances. The basic idea of the present paper is to explore a new approach of enhancing the compression system's aerodynamic performances by improving the time–space structure of the unsteady flow field.

### *2.2. The phenomenon of instantaneous reverse flow in the planar diffusion cascade flow field*

In order to explore directly the connection between the time-averaged performances and the unsteady vortex flow field, we would analyze the phenomenon of instantaneous reverse flow that is essential for the time–space structure of the unsteady flow field, starting from the fundamental "element", i.e. a planar cascade intercepted from the rotor blade row. Both experiments and CFD simulations were presented in [3], however only a set of CFD results will be quoted here to illustrate the instantaneous reverse flow that is closely connected with the unsteady vorticity field. Much number of this planar diffusion cascade flow is 0.5 with Reynolds number of $0.8324 \times 10^6$, the angle of attack is $6^\circ$ and $15^\circ$ and steady and uniform flow is assumed as the inlet boundary condition.

The CFD results demonstrated that there is a phenomenon of instantaneous reverse flow pervasive in the flow field. Take a fixed point above the trailing edge of the blade as an example, phase diagram of the velocity at this point is shown in Figure 1 for a period of time (the abscissa denotes the axial component of the velocity that coordinate the circumferential component and each point in the figure represents an instant). Positive values of the abscissa represent instantaneous forward flow and negative values of the abscissa represent instantaneous reverse flow. If the time period and the proportion of time period in which there occurs reverse flow are adopted respectively as the denominator and the numerator, then the fraction is defined as the reverse flow time ratio $\tau_{RF}$. The contour map of $\tau_{RF}$ for this cascade flow is shown in Figure 2, which gives the region where the instantaneous reverse flow occurs frequently, where the abscissa and the ordinate represent the axial and the circumferential directions.

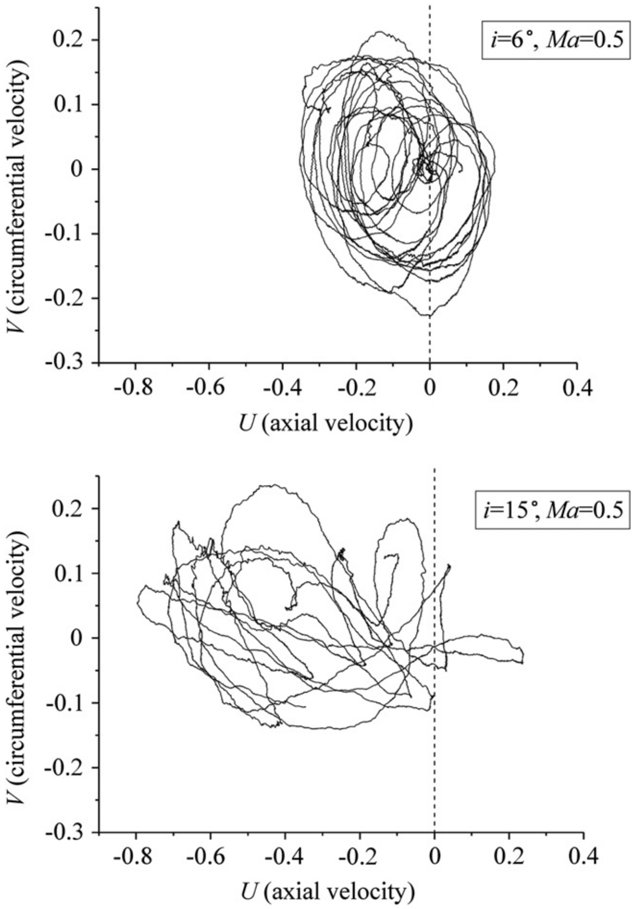


**Figure 1** Phase diagram of the velocity at the fixed point above the trailing edge of the planar diffusion cascade blade.

Indeed, the instantaneous reverse flow is a universal phenomenon in unsteady flow field with loss of reverse flow, rather than limited to the diffusion cascade flow. However, the unsteady vorticity flow inside the compression system has its specific characteristics. First, the instantaneous reverse flow here is closely related to the work-doing and the loss of the fluid flow, and secondly the reverse pressure gradient specific for the compression system exaggerates the phenomenon of instantaneous reverse flow. Finally, the phenomenon of instantaneous reverse flow relates closely with the compression system's aerodynamic instability and stall.

The present section will cover only the phenomenon of instantaneous reverse flow in the planar diffusion cascade, and its effect on the time-averaged aerodynamic performances will be described in Section 5 together with experimental verifications.

### *2.3. How to improve the time–space structure of the unsteady vorticity flow*

As mentioned in [4], if there are several bodies with relative motion present in the same flow field, this would

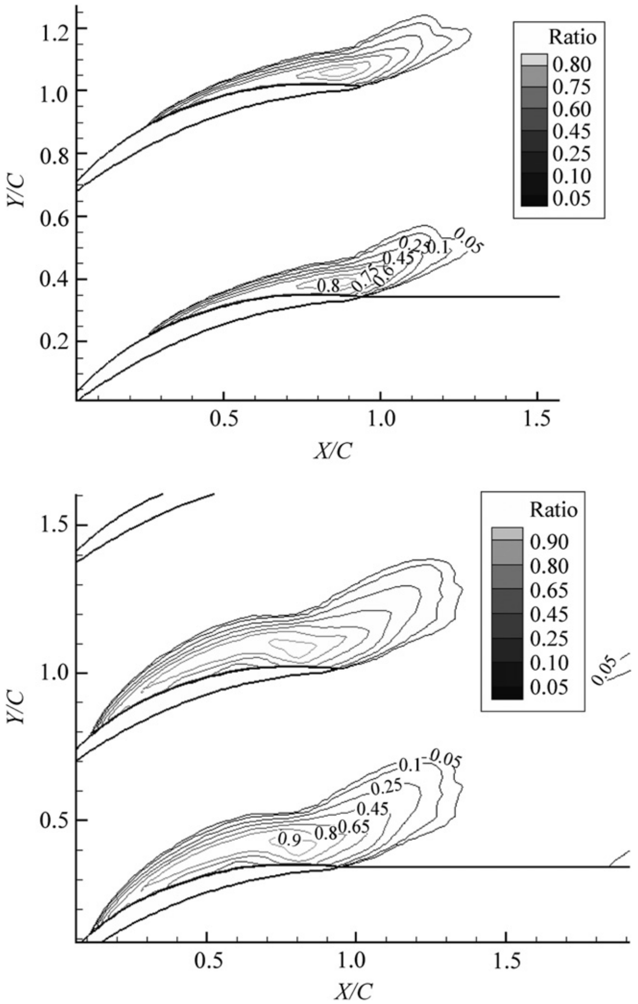


**Figure 2** Contour map of $\tau_{RF}$ (reverse flow time ratio) for the same cascade flow.

constitute a specific category of flows with certain common characters, one of which is the possibility of improving the time–space structures of these unsteady vortex flows, i.e. we can transform their random time–space structures into orderly ones by employing the inherent relative unsteady interactions between these moving bodies.

Migratory birds flying in formation is a typical example of this flow category. According to the experimental observation [5], in contrast with flying individually, the heart rate of pelican flying in formation will be decreased by 11.4%–14.5%, demonstrating the fact that the complex interactions between the unsteady wakes behind the upstream pelicans and the unsteady flows over the downstream pelicans have improved the time–space structures of the latter, and thus leading to energy saving. If the stagger arrangement of the rotor/stator within the compression system is compared to the migratory birds flying in formation, it might be deduced that there exists also a similar energy-saving approach for the compression system.

There are several co-axial rotating bodies with circumferential relative motion in the compression system, which can normally be classified into three groups. The first group, with the casing as its example, is static relative to the absolute coordinate system fixed on the casing; the second, with the fan rotor blade row as its example, is static relative to the cylinder coordinate system fixed on the low pressure axis; the third, with the high pressure compressor rotor blade row as its example, is static relative to the cylinder coordinate system fixed on the high pressure axis. If there are three axes in the system, the situation would be more complicated.

In accordance with the complexity of the structure of compression system, the time–space structures of the unsteady vortex flow field involved are also much complex. The randomness of the flow field is closely related with the complex interactions within the unsteady vorticity flow field, which has not, however, been taken into consideration in the current aerodynamic design of compression systems [6,7]. This is just the point we hope to realize breakthrough, i.e. improve the time–space structures of the flow field and realize the transformation from random into orderly. Efforts have been made in respect of theoretical analysis, CFD simulation and experimental observation to reveal and study the randomness of the time–space structure of these kinds of unsteady vorticity flow fields.

Particle image velocimetry (shortened to PIV) measurements were carried out in the flow field in an annular cascade wind tunnel for several angles of attack [8], the results showed that the unsteady vorticity strength varied greatly in the whole field and the spectrum was very complex at each point. The comparison between the time-averaged and the instantaneous vorticity field demonstrated clearly the inherent randomness. Analyses showed that the complexity lay in the fact that these kinds of flow fields were full of vortexes with different scaled vortex modes and broad frequency spectrum, and these vortexes kept on splitting and merging between different vortex modes, resulting in random time–space structure and the phenomenon of instantaneous reverse flow.

From the viewpoint of enhancing the time-averaged performances by improving the time–space structure, the key is properly changing the bodies' geometric shapes and parameters so that the time–space structure could be somewhat more orderly, and the main approach is exerting effective excitations on local flow fields to improve their original time–space structures. As shown in Figure 3, if excitations with proper frequencies and amplitudes are imposed on the unsteady vorticity flow field, the randomness of its time–space structure could be reduced. It can be seen from the comparison between Figure 3(a) and (b) that the instantaneous reverse flow is remarkably reduced and the total vorticity and parameters of quasi-vortex energy are improved [9,10]. From the time-averaged performances popular in engineering sector, the loss coefficient of the annular cascade is considerably decreased, as shown in Figure 4. Both Figures 3 and 4

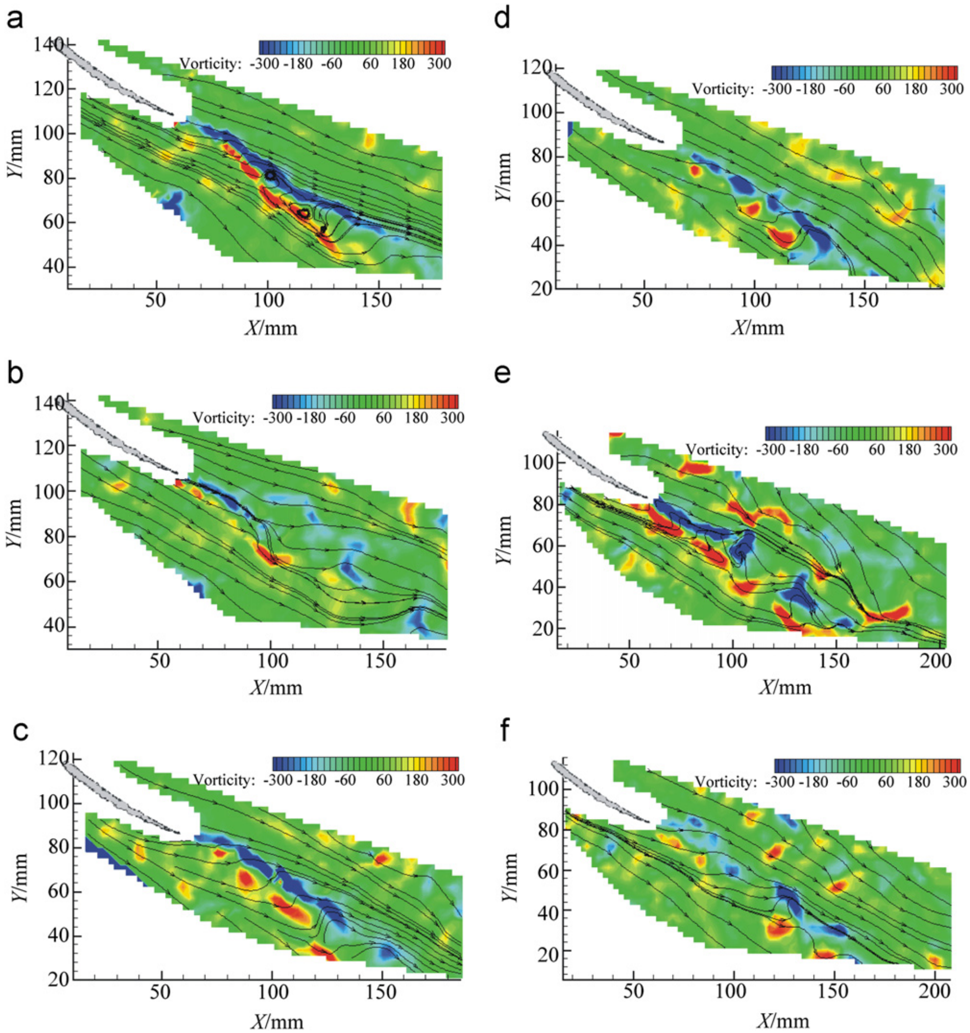


**Figure 3** PIV measurement of the instantaneous flow field in an annular cascade. (a) $i=5$ deg without excitation, (b) $i=5$ deg with excitation, (c) $i=10$ deg without excitation, (d) $i=10$ deg with excitation, (e) $i=16$ deg without excitation and (f) $i=16$ deg with excitation.

show that the time–space structure of the annular cascade is somewhat transformed from random into more orderly because of the effect of external excitations. Since this phenomenon results from the effect of external excitations on the time–space structure of the unsteady vorticity flow inside the annular cascade and this effect works only for a limited ranges of frequency and amplitude, it could thus be concluded that there occur certain coupling effects, and this kind of unsteady vorticity flows is called as "unsteady cooperative flow" (shortened to UCF). In contrast, the original unsteady vorticity flows without any improvement of time–space structure is called as "unsteady natural flow" (shortened to UNF) [11–13].

If the instantaneous reverse flow disappears completely in the whole flow field, this could be reckoned as a perfect unsteady cooperative flow field. This is an entirely ideal flow state with permanent zero time-averaged loss coefficient, but not realistic in the actual world. Hence the unsteady cooperative flow mentioned in the present paper implies only the fact that there is obvious improvement in the time–space structure (from random toward orderly) with obvious enhancement in the time-averaged performances.

## 3. Approach for improving time–space structure of unsteady vorticity flow field in compressor

### *3.1. How to exert unsteady excitations?*

#### *3.1.1. CFD simulations of different excitations imposed on the inlet boundary*

Take a planar diffusion cascade as example, three cases are simulated with nearly the same conditions, the unique difference lies in their inlet boundary condition. A is the case with a steady, uniform incoming flow; B and C are the cases where an unsteady excitation with different excitation frequencies are imposed on the inlet boundary condition. Reynolds averaged equations are adopted and the CFD simulation results give quite different phase diagrams on the velocity plane, as shown in Figures 5 and 6.

It can be seen from Figure 5 that Case B should be classified into UNF since there occurs severe instantaneous reverse flows, whereas Case C should be classified into UCF. Case A represents steady, uniform incoming flow condition without any excitations and there the instantaneous reverse flows are even worse than Case B, and thus be classified into UNF. At present, most CFD simulations of the planar diffusion cascade adopt steady uniform incoming flow as the inlet boundary condition, as in Case A, and their time–space structures are of the UNF type, leaving rooms for further improvements.

#### *3.1.2. Consideration from the boundary value problem of mathematical physics*

The results of a mathematical physics problem with three different boundary values are given in Figures 5 and 6 revealing that when the inlet boundary conditions are changed, the time-space structure could be changed from random toward somewhat orderly. Hence we could take the whole unsteady vortice flow field of compression system as the object to make further exploration.

As an example, the compression system of small passage-ratio turbo-fan engines consists at least of the subsequent sub-systems: (a) fan, (b) external passage, (c) high pressure compressor and (d) transition section between (a) and (c). From engineering viewpoint, if the whole flow fields are taken as the object, the research would be extremely difficult, since there are numerous bodies in relative circumferential motion involved, leading to numerous moving boundaries with numerous complex geometric parameters. It could be reckoned not possible, atleast for the time being, to analyze the whole compression system's flow field to design proper excitations to realize our goal. Hence, we would divide the whole flow field into several sub-regions and devise different approaches of excitations, and thus there would be several boundary value problems involved, which will be considered in the following sections.

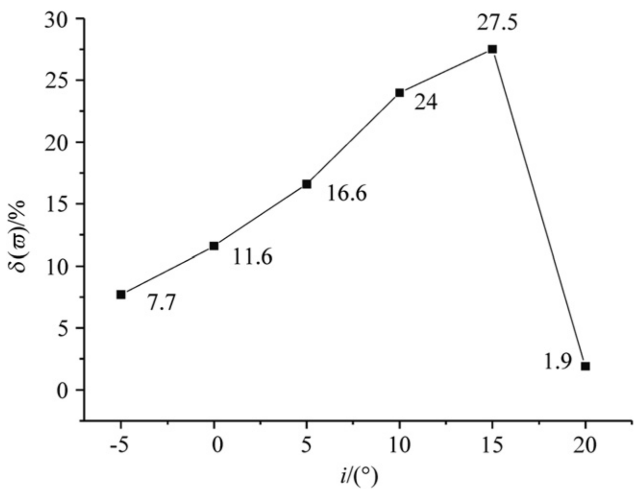


**Figure 4** Variation of the relative decrease of the annular cascade total pressure loss coefficient vs. the angle of attack.

### *3.2. Wake impact effects*

There have been many works concerning with the unsteadiness resulting from the stagger arrangement of rotor/stator, among which the unsteadiness of incoming flow over the upstream blade rows resulting from the coordinate system transformation are also well-known. "The wake impact effects" emphasized in the present paper are originated from and related to the transformation of random time–space structure of unsteady vorticity flow field into orderly one, and belong to a new regime of mechanism for energy-saving.

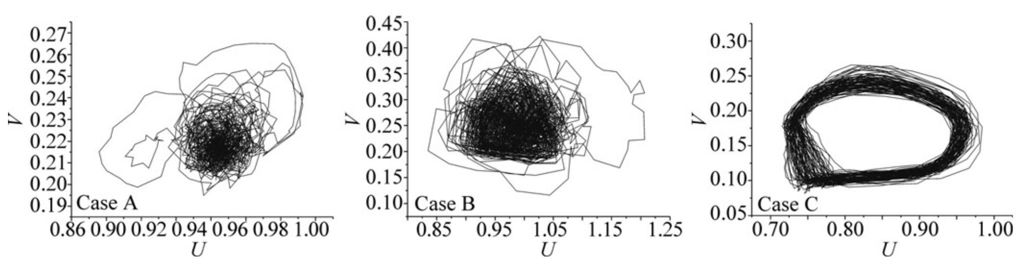


**Figure 5** Phase diagram on the velocity plane at a fixed point within the main stream of the planar diffusion cascade.

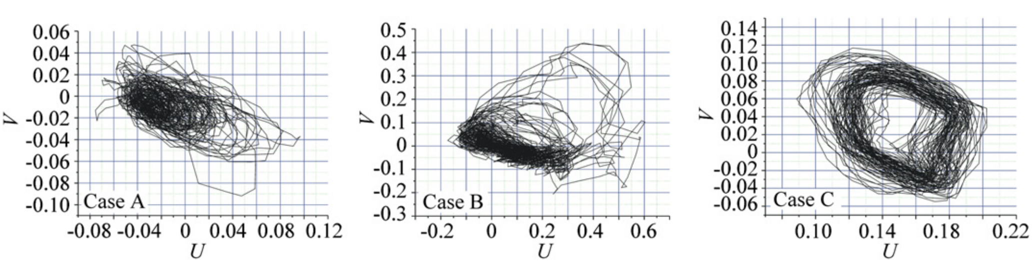


**Figure 6** Phase diagram on the velocity plane at a fixed point within the wake region of the planar diffusion cascade.

As for both rotor blade rows and stator blade rows, the time–space structures of their unsteady flow field are actually closely related to series of such geometric parameters as the blade number of the upstream blade row, i.e. the frequency spectrum characteristics of the upstream blade row is closely interrelated with and exerts significant influences on the time–space structure of the downstream blade row's unsteady flow field. This is why they are called "the wake impact effects".

As an example, the outlet flow from the upstream rotor blade row is non-uniformly distributed along the circumferential direction, after the transformation from the absolute coordinate system to the relative coordinate system, the downstream rotor blade row will thus experience an unsteady excitations coming from the upstream blade row, which will be called "the wake impact effects (WIE)". Under the action of WIE, there are two possibilities, one is no qualitative change occurs, the other is there appears an obvious transformation from random into somewhat orderly, i.e. from UNF into UCF, in the time–space structure of unsteady flow over the downstream blade row. Studies related to this effect are presented in [8,14–17], and relevant and positive experimental results for verifications will be presented in Section 4.

### 3.3. Proper excitations imposed at end regions

Presented in Section 3.2 is the arrangement for imposing unsteady excitations from the outlet of upstream blade row on the unsteady flow over the downstream blade row. The present section will discuss the excitations imposed at end regions, i.e. the excitations from regions related to both ends of the blade row. One common element shared with what mentioned in Section 3.2 is that the interaction between two bodies with relative motion in the circumferential direction is made use to exert the excitations.

Classified by the Mach number at the inlet of blade row, the present study covers three regimes. The first is the subsonic regime occurring in high pressure compressors, the second is the traditional transonic regime occurring in fans and high pressure compressors and the third is the complete transonic regime proposed recently in [18,19]. The traditional transonic is defined by the relative Mach number at the inlet of rotor and the stator blade row is not involved. In most cases, the absolute Mach number at the inlet of stator blade row is also subsonic. However, when the stage aerodynamic loading is further enhanced, there would be cases where the absolute Mach number at the stator blade root at the inlet is obviously supersonic, and in these cases the stator blade row would also be transonic as well as the transonic rotor blade row. Based on the above-mentioned, the stage consisting of transonic rotor blade row and transonic stator blade row was called the complete transonic stage in [19]. Since the stage loading is enhanced, the flow field around the stator blade root in the complete transonic stage is drastically deteriorated, and thus it is in urgent need to transform its time–space structure from UNC toward UCF.

With the above-mentioned three regimes as targets, exploration efforts have been made using two kinds of unsteady excitations.

The first is excitations imposed in end regions, focusing on the rotor blade tip region. The method of casing treatment has been widely applied to many models; however, no technical arrangement has yet been adopted to employ excitations distributed in the rotor flow field to improve the time–space structure of the unsteady flow over rotor. The end region excitations mentioned here are not the same as the casing treatment, and can be further divided into two classes. The first class has already witnessed improvements in the time–space structure; it has some similarity with the casing treatment, however, there are several changes both in geometric parameters and in structure. The second class is asymmetric and is thus called "the blade tip excitation generator", and has also collected positive results in experimental verifications, as described in Section 4.

In addition to the end region excitations, the second is a new idea aiming at improving the time–space structure of the casing unsteady flow field, named as "the casing unsteady excitation generator", and positive results have also been reported in annular cascade wind tunnel experiments [20].

### 3.4. Asymmetric excitations

One of the Nature's complexities is that many phenomena are merging of the symmetric and the asymmetric, e.g. the face of normal people is not strictly symmetric, neither is the aero-compression system. With symmetrically structured construction, there would still appear series of asymmetric phenomena in actual operation, e.g. the occurrence of rotating stall implies the transition from a stable symmetric flow state to an asymmetric flow state [21]. Circumferential distortion of the incoming flow leads to earlier occurrence of rotating stall, which could be thought of as the result of interactions between two kinds of asymmetric flows. When there occurs stall flutter in the fan blade row, the rupture of blade is asymmetrically distributed in the circumferential direction, which is closely related to asymmetric distribution of the phase angles between blades [5,11], and much more examples of asymmetric phenomena could be enumerated.

Studies on the implementation of asymmetric excitations are mainly carried out in two directions. One is the above-mentioned asymmetric "blade tip excitation generator", which could produce positive results for symmetric incoming flow [22]. Another is how to use asymmetric excitations to solve problems brought about by asymmetric incoming flow [22], which was also somewhat verified in experiments.

The second kind of asymmetric excitations is called "the design method of unsteady axial aerodynamic layout for asymmetric stator blade rows", i.e. the original symmetric layout of guide vanes and stator blade rows is changed into asymmetric layout, aiming at imposing asymmetric excitations on the unsteady flow over downstream rotor blades to improve its time–space structure.

### *3.5. Comparison study of the counter-rotating and the co-rotating compression systems*

In later 90s, we carried out experimental studies on the unsteady vorticity flow in counter-rotating compression systems using a counter-rotating mine fan facility [23]. The results showed that the counter-rotating fan has higher efficiency and broader working range than the co-rotating fan.

As for the development of turbofan engines, the studies on unsteady cooperative flow will be focused on the engineering applications of low pressure and high pressure counter-rotating machines. Experimental studies of [23] were concerned with the unsteady flow in the flow chamber between two counter-rotating rotors. The results showed that the time–space structure of the flow in the chamber reflected potential disturbances form the downstream rotor, as well as the influences of the wake impacts from the upstream rotor, and thus we can not use the normal periodic condition to analyze the unsteady vorticity flow in the chamber.

A new model was proposed in [24,25] to analyze the sub-domain of chamber between the rotor blade row and the stator blade row. In the new model, the traditional method is adopted for the upstream and the downstream blade row, i.e. only one passage is considered as a sub-domain, whereas the whole chamber between the two blade rows is considered as an indivisible sub-domain, since the traditional periodic condition can not be applied. A new computational scheme is also devised, in which the asymmetry of at the inlet and outlet of each sub-domain is taken into consideration. The new scheme facilitates, on one hand, the comparative study between co-rotating and counter-rotating compression systems by offering CFD simulation software. On the other hand, it makes possible the enhancement of the time–space structure of unsteady vorticity flow fields.

**Table 1** Improvement of performances by UCF design.

| Performances | Base design | UCF design | Enhancement/% | |
|---|---|---|---|---|
| | | | Absolute | Relative |
| $\pi_C$ | 6.51 | 7.02 | 0.51 | 7.82 |
| $\eta_C$ | 0.85 | 0.89 | 0.04 | 5.26 |

### *3.6. Example of the aerodynamic design of multi-stage axial compressor improved by UCF*

Take the standard aerodynamic design of a 5-stage axial compressor as the base for further improvement by using UCF. The standard aerodynamic design proceeds as follows: (1) Preliminary 1D and 2D aerodynamic design and geometric parameters. (2) Commercial software is employed to carry out 3D N-S Code simulation of the whole compressor. (3) Repeatedly revise the preliminary design till a satisfactory design is obtained and this design proposal will be adopted as the base for the UCF-improved aerodynamic design.

The goal of UCF-improved design is to promote the transformation of time–space structure of 5 unsteady flows over the 5 rotor blade rows from random toward orderly and this design can be divided into two steps.

First, the following manipulations should be carried out for each of the 5 rotors. (1) Use unsteady N-S Code to simulate the unsteady flow over the rotor. (2) Try different layout design of impose unsteady excitations. (3) Use unsteady N-S Code to re-simulate the unsteady flow with imposed unsteady excitations. (4) Compare and analyze the time-averaged performances before and after the imposition of unsteady excitations.

Second, input the new time-averaged performances into the aerodynamic layout design software for multi-stage compressor so that the overall effects of the UCF design can be evaluated. These two steps should be repeated till the results are converged. The comparisons of performances at the design condition before and after

**Table 2** Block diagram of the UCF design of multi-stage compressor.

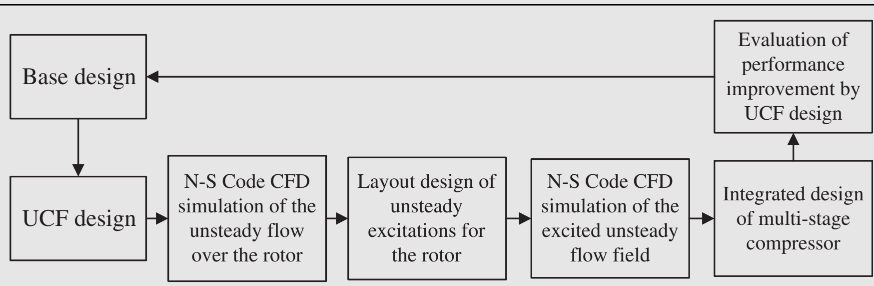

the UCF design are listed in Table 1. Schematic block diagram of the UCF design is shown in Table 2.

## 4. Experimental verification

### 4.1. Objectives of the experimental verifications

(1) Series of improvements are proposed in Section 4 based on the concept of 'UCF in CS' which is preliminarily verified by CFD simulations. However, the concept will be taken as an assumption only if it can not be verified by experiments at the level of basic research. Therefore, experimental verifications are devised and conducted, with emphases laid on implementing the improvements of time-averaged performances $\{\pi:\eta:SM\}$ which are significant and of practical importance.
(2) The unsteady vorticity fields before and after the implementation of improvements are compared and used to analyze the relationship between the enhancement of time-averaged performances and the improvement of unsteady vorticity fields.

### 4.2. Verification of wake impact effects (WIE)

#### 4.2.1. Experimental verifications of optimal coupling scheme for WIE

In experiments, we first measured the unsteady vorticity field at the outlet of compressor rotor row, and obtained the prevailing vortex shedding frequency as $f_{shed}=1854$ Hz. The present paper will analyze the influence of wake impacting frequency on the compressor's performances and aerodynamic stability, rather than elaborate the specific measurements and analysis which can be found in [14].

The optimal condition with design operational rotating speed and uniform inlet condition (the wake impacting frequency $\bar{f}_e=0$) is chosen as the benchmark for the comparison. Variations of the compressor's efficiency and total pressure rise vs. the excitation frequency are examined, the influence of the excitation frequency on the compressor's stall margin is analyzed and the experimental results are shown in Figures 7 and 8.

As shown in the figures, the compressor's total pressure rise is increased by the wake impact effect, whereas its impact on compressor's efficiency is not so clear-cut. In comprehensive consideration of the efficiency and total pressure rise, i.e. on the basis of increasing the total pressure rise while keeping the adiabatic efficiency basically not decreased, the effective range of excitation frequency is obtained as $0.6\leq\bar{f}_e\leq1.2$ (the region limited by two blue vertical lines shown in Figure 7). Within this region, the total pressure rise is considerably increased while the compressor's efficiency is basically unchanged, with the former reaching its peak at $\bar{f}_e\approx1.0$. When $\bar{f}_e>1.2$, the total pressure rise is increased somewhat, while the compressor's efficiency is significantly reduced. Variation of the compressor's relative increment of stall margin vs. the wake impacting frequency is given in Figure 8, from which it can be seen that at most excitation frequencies, WIE can increase the compressor's stall margin with its peak occurring at $\bar{f}_e=1.0$.

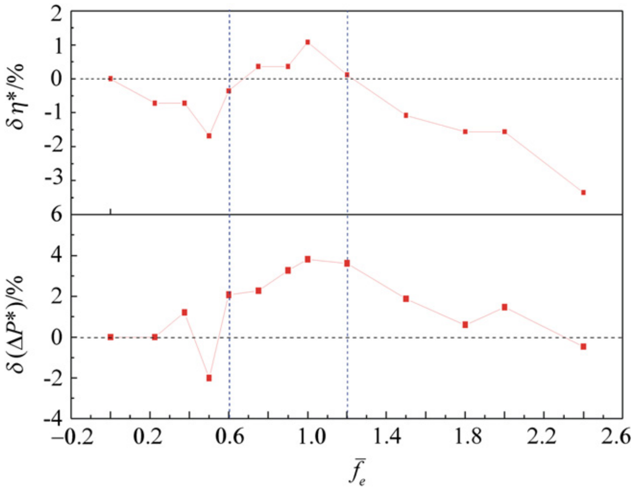


**Figure 7** Variations of the efficiency and total pressure rise vs. the excitation frequency at the design operation condition.

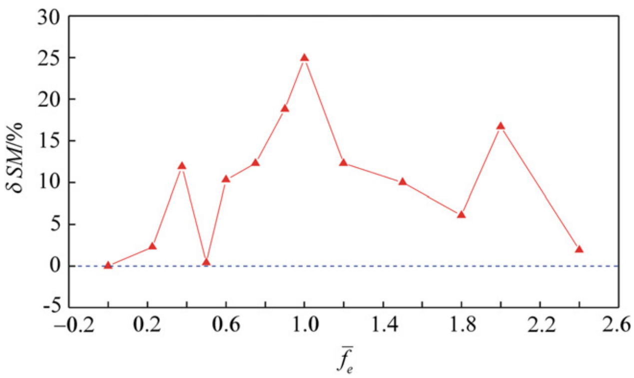


**Figure 8** Variations of the stall margin vs. the wake impacting frequency.

Table 3 presents experimental data of the compressor's total pressure rise, efficiency and stall margin at the design operation condition corresponding to different wake impacting frequencies.

In summary, $0.6\leq\bar{f}_e\leq1.2$ is the effective (nondimensional) wake impacting frequency range and $\bar{f}_e\approx1.0$ is the optimal WIE coupling scheme.

#### 4.2.2. Influence of WIE on the compressor's performances

All the above-mentioned works were carried out at $\bar{n}=100\%n_d$, however actual engines are regularly working at varied rotational speed and mostly in the range of 80%–90 % of the design rotating speed. Hence it is necessary to validate the optimal excitation frequency at varied rotational speed as described below.

Characteristics of the compressor under the optimal excitation frequency and working at different rotational

**Table 3** Influence of the wake impacting frequency on the compressor's performance and stall margin.

| $\bar{f}_e$/Hz | $\dot{m}_d$ | | | | $\dot{m}_{stall}$ | | |
|---|---|---|---|---|---|---|---|
| | $\Delta(\Delta P^*)$/Pa | $\delta(\Delta P^*)$/% | $\Delta\eta^*$/% | $\delta\eta^*$/% | $SM$/% | $\Delta SM$ | $\delta SM$/% |
| 0 | 0 | 0.00 | 0.0 | 0.00 | 26.1 | 0.000 | 0.0 |
| 0.23 | 0 | 0.00 | −0.6 | −0.72 | 26.7 | 0.006 | 2.3 |
| 0.38 | 18 | 1.21 | −0.6 | −0.72 | 29.2 | 0.031 | 11.9 |
| 0.50 | −30 | −2.01 | −1.4 | −1.68 | 26.2 | 0.001 | 0.4 |
| 0.60 | 31 | 2.08 | −0.3 | −0.36 | 28.8 | 0.027 | 10.3 |
| 0.75 | 34 | 2.28 | 0.3 | 0.36 | 29.3 | 0.032 | 12.3 |
| 0.91 | 49 | 3.28 | 0.3 | 0.36 | 31.0 | 0.049 | 18.8 |
| 1.00 | 57 | 3.82 | 0.9 | 1.08 | 32.6 | 0.065 | 24.9 |
| 1.21 | 54 | 3.62 | 0.1 | 0.12 | 28.9 | 0.032 | 12.3 |
| 1.51 | 28 | 1.88 | −0.9 | −1.08 | 28.7 | 0.026 | 10.0 |
| 1.81 | 9 | 0.60 | −1.3 | −1.56 | 27.7 | 0.016 | 6.1 |
| 2.01 | 22 | 1.47 | −1.3 | −1.56 | 30.4 | 0.043 | 16.7 |
| 2.42 | −7 | −0.47 | −2.8 | −3.35 | 26.6 | 0.005 | 1.9 |

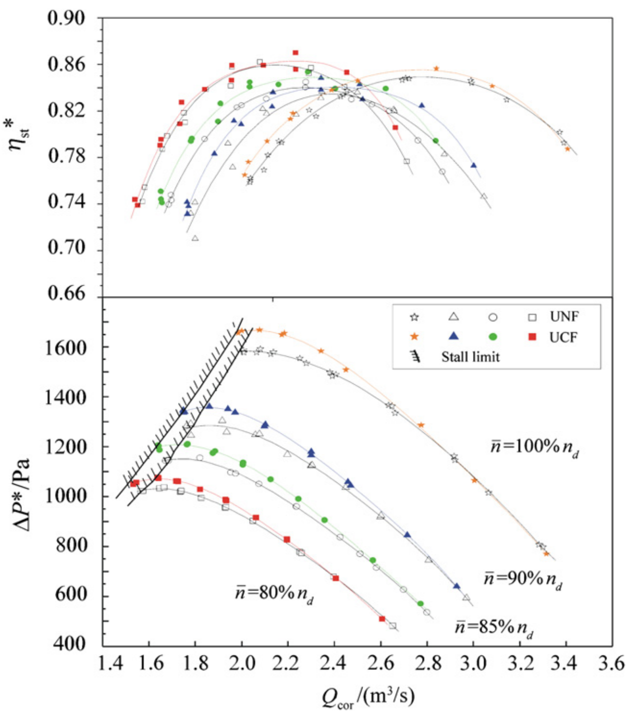


**Figure 9** Influence of WIE on the compressor's time-average performances at different rotating speeds.

speeds are given in Figure 9. As shown in the figure at the four measured rotational speeds, the unsteady WIE can always increase the compressor's averaged performances and stall margin. And thus it can be concluded that even when the rotational speed is changed the unsteady WIE can still be locked on the above-mentioned optimal excitation frequency. However, as the rotational speed is reduced, WIE's relative amplitude of the upstream blade row is also reduced and the coupling effect is thus reduced. As shown in Figure 9, when $\bar{n}=80\%n_d$, the gain from WIE is remarkably decreased.

**Table 4** Influence of WIE on compressor's performance at different rotating speeds.

| $\bar{f}_e$ | Parameters | $\bar{n}$ | | | |
|---|---|---|---|---|---|
| | | $100\%n_d$ | $90\%n_d$ | $85\%n_d$ | $80\%n_d$ |
| 0.0 | $\Delta P_d^*$/Pa | 1592 | 1285 | 1152 | 1037 |
| | $\eta_d^*$/% | 84.5 | 82.1 | 83.0 | 85.0 |
| | $SM$/% | 26.1 | 28.9 | 30.8 | 31.0 |
| 1.0 | $\delta(\Delta P_d^*)$/% | 4.52 | 5.84 | 4.95 | 3.95 |
| | $\delta(\eta_d^*)$/% | 1.53 | 2.87 | 1.92 | 0.25 |
| | $SM$/% | 32.6 | 34.9 | 40.3 | 35.5 |
| | $\Delta SM$/% | 0.065 | 0.060 | 0.095 | 0.045 |
| | $\delta SM$/% | 24.9 | 20.2 | 30.7 | 14.5 |

As shown in Figure 9, when $\bar{n}=85\%$, $90\%n_d$, the compressor's time-averaged aerodynamic performances are significantly enhanced, the efficiency, total pressure rise and stall margin are all improved. Refer to Table 4 for specific data.

### 4.2.3. *Influence of WIE on the time–space structure of the compressor's flow-field*

In order to further analyze evolution of the time–space structure of the compressor's flow-field, PIV experiments on its internal flow field are conducted, and two vortex system structures of the rotor's flow fields at nearly stall condition are compared, one corresponds to the uniform inlet flow and the other corresponds to the optimal WIE. In this way the evolution of the compressor's flow-field structure and the mechanism underlying the enhancement of time-averaged performances and stall margin by UCF are revealed and clarified.

The averaged vorticity distribution of the rotor flow-field corresponding to the uniform inlet flow is given in Figure 10(a), while the averaged vorticity distribution

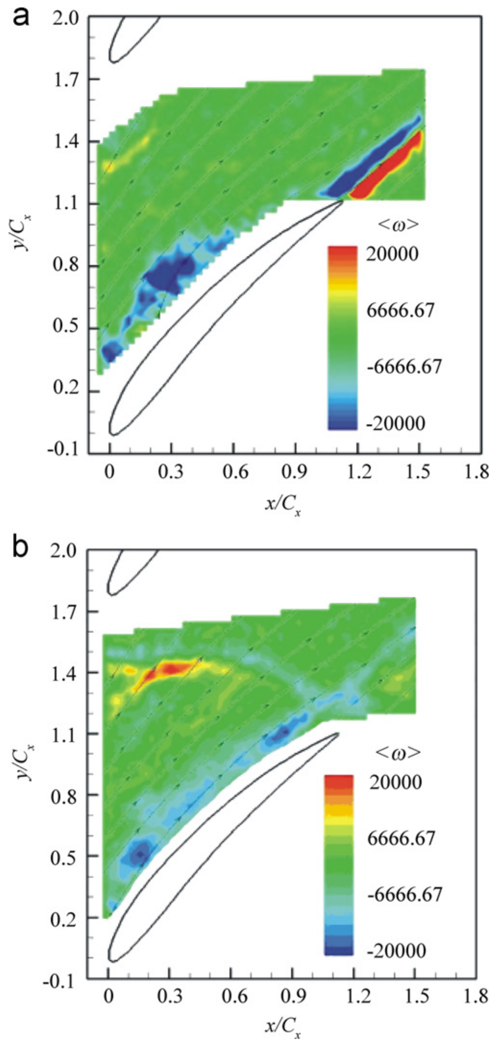


**Figure 10** Time-average vorticity distribution of rotor blades' suction section in different flow regime. (a) UNF and (b) UCF.

of the rotor flow-field under the optimal wake impact condition ($\overline{f}_e = 1.0$) is shown in Figure 10(b).

As shown in the figure, the vorticity in the rotor blade row's unsteady separated flow is greatly reduced on the suction side under the coupling effects of the upstream blade row's wake, and Karman vortex street is effectively restrained at the compressor's rotor blade trailing edge. In other words, the compressor's rotor blade row's flow-field is more regularly and orderly and this is the physical mechanism underlying the enhancement of time-averaged performances and stall margin when UNF is transformed into UCF.

### 4.3. *Experimental verification of the end-region excitation*

As for complex flow in the compressor's end region, coupling excitation experiments are carried out in blade tip region at both low and high speed as well as experiments for verifying casing coupling excitation. In the former case, similar results are obtained for both low and high speed and only high speed results are presented here.

#### 4.3.1. *Experiment results of blade tip coupling excitation*

Based on empirical design of casing treatment, optimal design of excitation frequency and excitation location is performed to facilitate the transformation from UNF into UCF in the end region flow, and verification experiments are carried out on a transonic single stage compressor, the results of which are shown in Figure 11(a) and (b) [26].

As shown in the figure, when the blade tip coupling is implemented, the compressor's stall boundary is shifted to lower flow rate under the experiment conditions, the stall margin is improved, the compressor's efficiency is enhanced near the peak efficiency, and the new casing treatment can increase the compressor's adiabatic efficiency at large flow rates. It is worth noting that at large flow rates (88%–98%) the new coupling can greatly improve the compressor's adiabatic efficiency and stall margin: increasing the adiabatic efficiency by 0.3% while

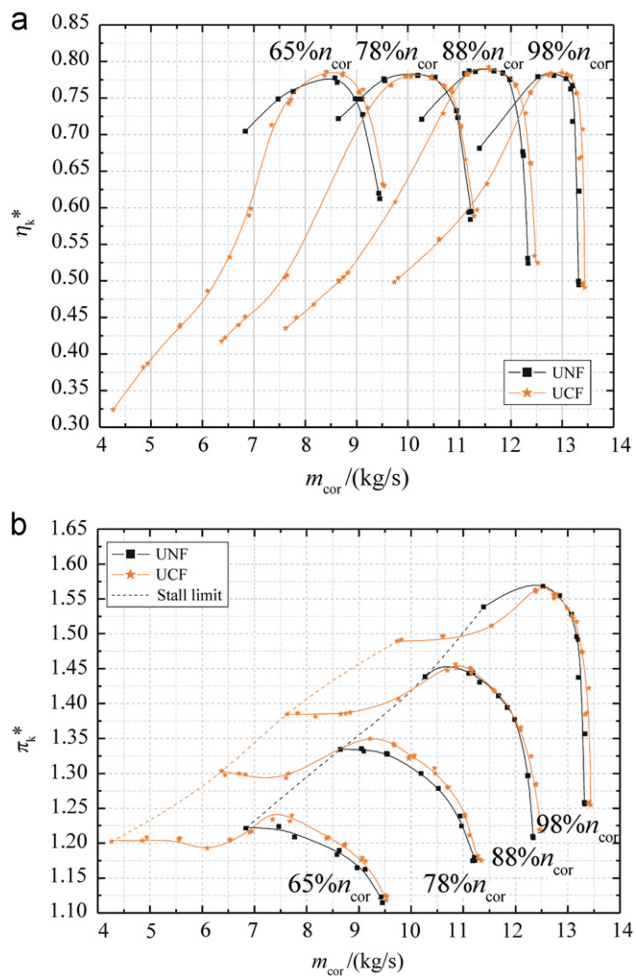


**Figure 11** Influence of (generator of blade tip excitation) GTE on transonic compressor's time-average performance. (a) Efficiency curves and (b) total pressure ratio curves.

enhancing the stall margin by 20%, i.e. implementing positive results of "improving stability while increasing efficiency" on transonic compressors.

It can be concluded that after optimizing the empirical design of casing treatment, the multiple vortexes system in the compressor's blade tip flow field can be rectified to facilitate the transformation from UNF into UCF. And thus the strength of leaking vortexes is decreased, the loss and blockage effects in the end flow region are reduced, aerodynamic loading at the leading edge of rotor blade tip is effectively decreased so that the compressor's efficiency and stall margin are remarkably improved.

### 4.3.2. Experiment results of casing coupling excitation

As for corner region separation in the high loading stator blade row flow field near the casing, experimental verification of the casing coupling excitation was performed on a low speed angular cascade, and influences of the casing excitation on the stator blade row flow field and related performances were analyzed as follows.

I. Influence of the casing excitation on the cascade outlet flow-field.

Total pressure recovery coefficient distributions on the annulus cascades' outlet section are given in Figure 12(a) and (b) for the cases of solid casing and casing excitation. It can be seen from Figure 12(a) that the flow blockage resulting from leaking vortexes at the blade root brings about flow separation in a relatively large scale at the cascade outlet, shown as blue low speed region in the figure. As shown in Figure 12(b), the casing excitation reduces remarkably the low speed region near the casing at the cascade outlet, while the blade wake is respectively broadened, especially from the middle of blade up to the casing. And thus, the casing coupling excitation can effectively improve the flow blockage resulting from leaking vortexes in the end region at the cascade outlet.

Hence it can be concluded that when the excitation frequency is coupled with the characteristic frequency in the separation region near the cascade blade root, the internal flow-field would be transformed somewhat from UNF into UCF, and thus the flow separation in the cascade's corner region is effectively restrained, the flow blockage is relieved and the internal flow-field structure is greatly improved.

II. Influence of the casing excitation on the cascade performances

In order to analyze the influence of casing excitation on the cascade's performances, radial distributions of the total pressure recovery coefficient at the cascade outlet are compared and analyzed, as shown in Figure 13.

As shown in the figure, for the benchmark case, the flow blockage was rather severe in the cascade end region, extending from the blade root to nearly 60% of the blade height. On the other hand, for the case of casing excitation, the coupling between the casing excitation and the separation vortexes in the cascade corner region reduces effectively the strength of the vortexes leaking through the clearance and reduces the low speed region resulting from the leaking vortexes. And thus the flow in the end region is greatly improved and the total pressure recovery coefficient is enhanced significantly.

### 4.4. Experimental verification of non-axisymmetric coupling mechanism

The blade tip coupling was adopted to carry out experimental verifications on our low speed and high

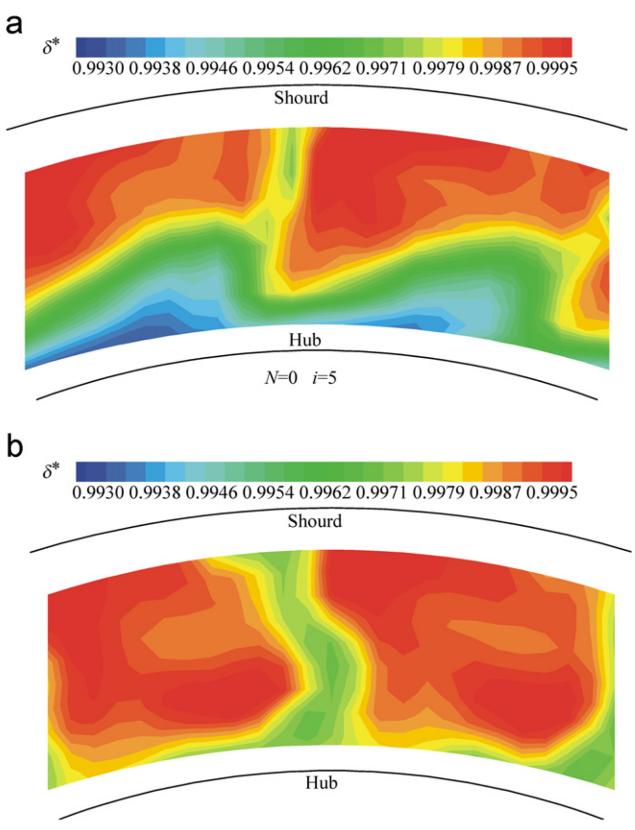


**Figure 12** Total pressure distribution on the annulus cascades' outlet section at different hub rotating speeds. (a) UNF and (b) UCF.

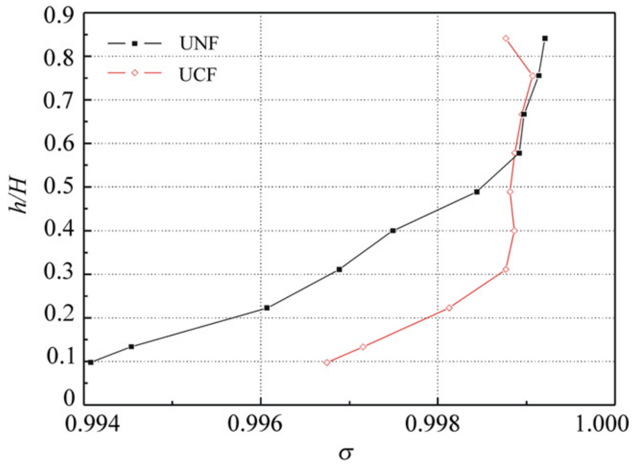


**Figure 13** Radial distribution of $\sigma = P_2^*/P_1^*$ at annulus cascades' outlet flow fields.

speed compressors, and the results are presented here.

### 4.4.1. *Experimental verification of non-axisymmetric blade tip excitation at uniform inlet flow*

I. Experimental verification of low speed asymmetric blade tip coupling excitation

Based on the above-mentioned scheme of optimal excitation frequency, the axisymmetric blade tip excitation scheme was further optimized by adopting non-axisymmetrical circumferential layout, and experiments were conducted at $\overline{n} = 85\%\ n_d$, at which the symmetric case attained its best result. Figure 14(a)–(c) gives respectively the compressor's efficiency and total pressure rise for the cases of solid casing, axisymmetric GTE and non-axisymmetric GTE.

As shown in the figure, the axisymmetric blade tip coupling excitation can significantly increase the compressor's total pressure rise and stall margin, which is, however, acquired at the cost of decreasing its adiabatic efficiency. On the other hand, the non-axisymmetric scheme can, in comparison with the case of solid casing, not only increase the compressor's total pressure rise and stall margin but also keep its peak efficiency not decreasing, in fact increasing by 1%. An especially at large flow rate, the maximum increment of efficiency attains 1.8%, as shown in Table 5.

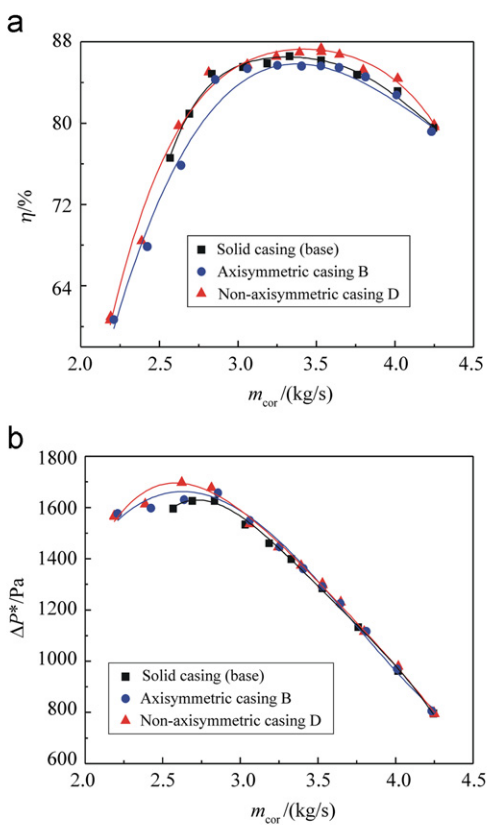


**Figure 14** Influence of casing's structure on low-speed compressor's performance. (a) Efficiency curves and (b) total pressure ratio curves.

**Table 5** Influence of axisymmetric and non-axisymmetric GTE on low-speed compressor's performance.

| Casing type | $\eta^*_{\max}/\%$ | $\Delta P^*_{\max}/\text{Pa}$ | $\Delta SM$ |
|---|---|---|---|
| Baseline | 86.5 | 1607 | 0.00 |
| Symmetric GTE | 85.8 | 1627 | 0.24 |
| Asymmetric GTE | 87.5 | 1636 | 0.24 |

II. Experimental verification of high speed non-axisymmetric blade tip coupling excitation

Relative to the coupling frequency prevailing in the axisymmetric blade tip excitation scheme, the non-axisymmetric blade tip excitation scheme with non-axisymmetrically circumferential layout will generate broadened frequency band, which will more effectively improve the structure of complex flows in the compressor's end region, resulting in better time-averaged performances and stability. In order to verify its applicability to transonic compressors, series of experiments was carried out, in which the high speed axisymmetric blade tip excitation scheme was optimized by incorporating experiences gained from the low speed non-axisymmetric experiments. And thus optimized non-axisymmetric blade tip excitation scheme was devised, and experimental verification was performed for 4 operation conditions: $\overline{n} = 65\%$, 78%, 88%, 98%$n_d$ as shown in Figure 15.

In comparison with the axisymmetric scheme, although the non-axisymmetric scheme leads to a slightly lower stall margin (it is still 10%–17% better than the unexcited case), however it shows better capability in enhancing the compressor's time-averaged performances, in particular increasing its peak efficiency by 1.3% at the design operation condition. Refer to Table 6 for specific data.

It can be concluded from the above-mentioned that the non-axisymmetric blade tip excitation scheme can generate broader coupling frequency band to realize the action of 'coupling and regulating' upon different-sized vortex systems, resulting in lower loss and better performances.

### 4.4.2. *Experimental verification of non-axisymmetric blade tip excitation at distorted inlet flow*

The above-mentioned is for the case of uniform inlet flow, if the inlet flow is distorted, the inlet condition would be greatly non-axisymmetric and the compressor's time-averaged performances and aerodynamic stability would be deteriorated. How to arrange the end region excitation to deal with the distortion and facilitate the desired coupling is our new objective.

At present, experimental verification was completed for blade tip axisymmetric and non-axisymmetric excitations imposed on low speed axial flow compressors. As shown in Figure 16, optimization of the blade tip coupling excitation devise by using UCF theory can effectively enhance the compressor's stall margin at distorted inlet flow, which is increased by 74.7% and 47.7% for axisymmetric and non-axisymmetric coupling, respectively.

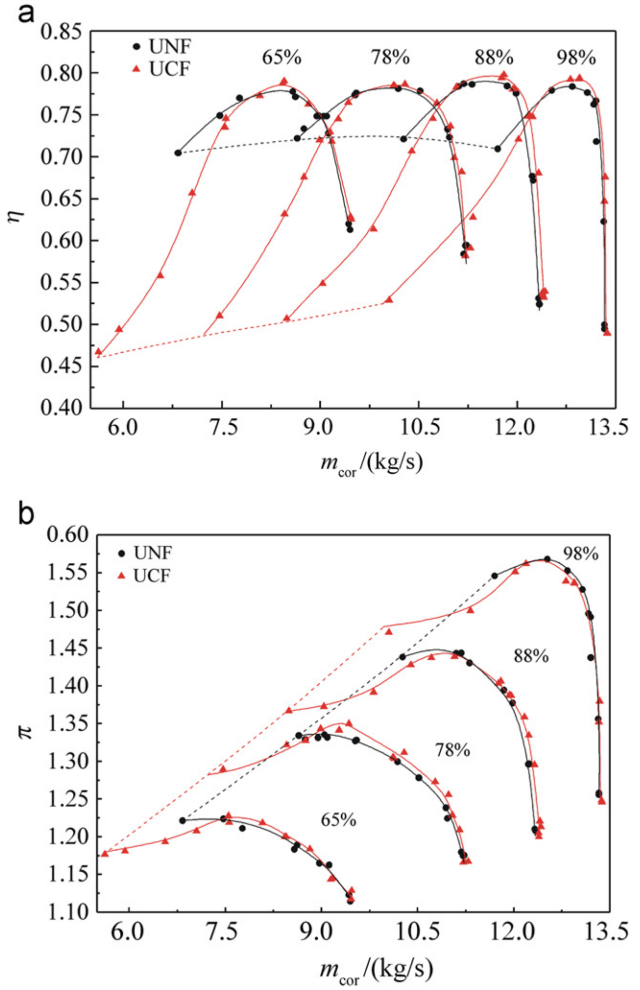


**Figure 15** Influence of non-axisymmetric GTE on transonic compressor's performance. (a) Efficiency curves and (b) total pressure ratio curves.

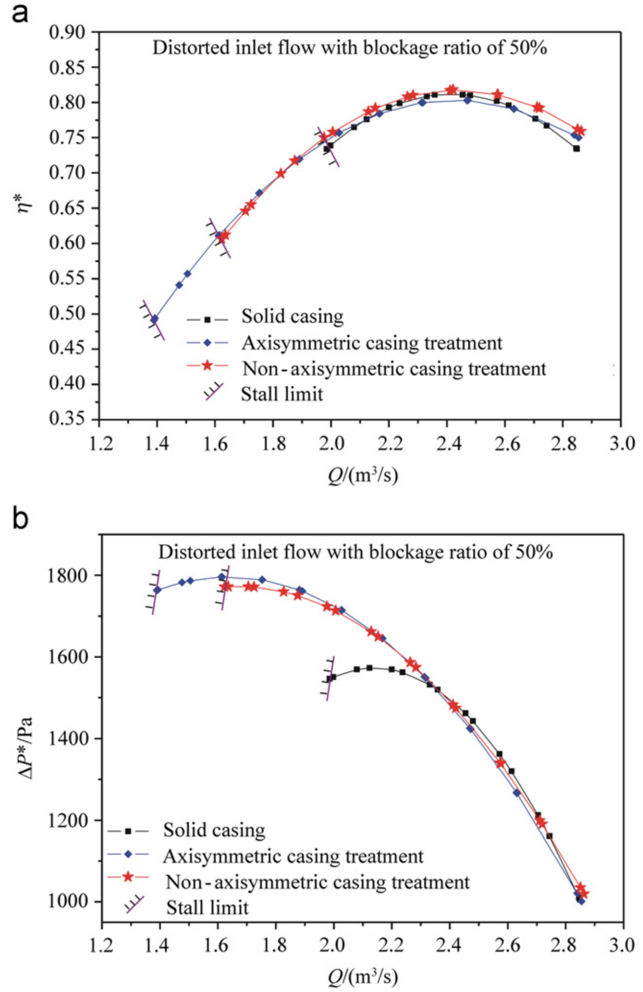


**Figure 16** Influence of non-axisymmetric GTE on low-speed compressor's performance at distorted inlet flow. (a) Efficiency curves and (b) total pressure ratio curves.

**Table 6** Influence of non-axisymmetric GTE on compressor's performance.

| Correct rotating speed | $\Delta SM$ | $\Delta\eta^*_{\max}$/% |
|---|---|---|
| $\bar{n} = 65\% n_d$ | 0.175 | 1.07 |
| $\bar{n} = 78\% n_d$ | 0.118 | 0.71 |
| $\bar{n} = 88\% n_d$ | 0.149 | 0.94 |
| $\bar{n} = 98\% n_d$ | 0.107 | 1.28 |

The axisymmetric coupling scheme is more powerful in dealing with the distorted inlet flow, however, the efficiency is slightly reduced (it is decreased by 0.7% at the design condition). In contrast, although the non-axisymmetric coupling one is less effective in dealing with distorted inlet flow (the stall margin is increased by 47.7%, a result not so bad), it can, however, increase the efficiency by 0.7%.

It can be concluded that at distorted inlet flow, well-organized blade tip excitation can still effectively improve the internal flow field structure. Specifically, it can enhance the compressor's stall margin and total pressure rise while increase its efficiency so that both the compressor's time-averaged performances and the flow stability can be enhanced.

## 5. Conclusions

### *5.1. The concept of 'UCF in CS' is briefly summarized as follows*

(1) When there are several bodies with relative motion in a flow field, the flow field is classified as a special one [6], and the flow in the compression system of modern aero-engine is one of its example.
(2) One common feature of the above-mentioned flows is that the unsteady interaction between those bodies with relatively motion can be use to facilitate the transformation of the time–space structure of part flow field from random toward orderly.

(3) The fundamental function of a compression system, i.e. doing work to boost the pressure, is closely related to the quality of its unsteady flow field, since the time–space structure of the unsteady vortice flow field will affect the time-averaged aerodynamic performances of the compression system.
(4) The quality of the flow field's time–space structure can be described via different approaches; however, it is found that the quality can be most instinctively reflected by the phenomenon of instantaneous reverse flow.
(5) The annular cascade wind tunnel experiments showed that external excitations can be use to facilitate the time–space structure of the cascade unsteady flow field to transform from random toward orderly, which is brought about by the coupling effect between the external excitations and the internal flow field.
(6) Based on the experimental results, the concept of "Unsteady Cooperative Flow in Compression System" (shortened to UCF in CS) was proposed. When the flow type is transformed from Unsteady Natural Flow toward Unsteady Cooperative Flow, its time–space structure is transformed from random toward orderly, which will lead to remarkable improvement in the time-averaged aerodynamic performances of the compression system.

## 5.2. Experimental verifications of the proposed technical arrangements

Experiments were carried out to validate series of proposed arrangements of excitations under actual rotating conditions, attempting mainly to check the improved performances of a single stage axial compressor. The experiments were carried out on a low speed axial compressor and a single stage transonic compressor, and the main results are summarized as follows.

### 5.2.1. Wake impact effects

Experiments were repeated on a low speed axial compressor. Geometric parameters of the upstream guide vane ahead of the rotor were adjusted to obtain improved time-averaged performance, which was thought of as the positive results in the transformation of time–space structure. Under the design condition, the relative enhancements in the isentropic efficiency, the total pressure and the stall margin are 2.26%–3.60%, 4.40%–6.0% and 20.4%–25.6%, respectively.

### 5.2.2. End region excitations

There are different structures and several parameters involved in the end region excitations, classified into two categories, i.e. axisymmetric and non-axisymmetric excitations in the circumferential direction. Relevant experiments were carried out on the two compressors for verification, and the time-averaged performances were improved, as shown in Tables 7 and 8.

### 5.2.3. Arrangement of end region excitations at distorted inlet flow

When there is circumferential distortion in the inlet flow, the time-averaged performances of axial compressors will be drastically deteriorated, and how to arrange the end region excitations to realize desired improvements is our main purpose. Experiments were mainly carried out on the low speed axial compressor and the results are listed in Table 9.

## 5.3. Problems to be further studied

(1) The time–space structure of CS internal flow has multi-scale characteristics. However, the present study aims at improving CS's performances, therefore only those factors that have strong influences on its time-averaged performances are considered in devising simplified physical-mathematic model, which will impact CFD, experimental schemes and technical detail and is still in the process of perfection.
(2) In CS internal flow-field, the factors exerting strongest influence on the transformation from UNF into UCF are the chamber between the rotor blade row and the stator blade row and the end region near the rotor and stator blades, relevant studies are far from completed.

**Table 7** Experiment results on a low speed compressor.

| Time-averaged performance | Excitation | Designed condition | |
|---|---|---|---|
| | | $\Delta$ | $\delta/\%$ |
| $\Delta P^*$ | Symmetric | 20 Pa | 1.24 |
| | Asymmetric | 20 Pa | 1.24 |
| $\eta$ | Symmetric | −0.7 | −0.8 |
| | Asymmetric | 1.0 | 1.2 |
| $SM$ | Symmetric | 0.242 | 117.5 |
| | Asymmetric | 0.241 | 117.0 |

**Table 8** Experiment results on a single stage transonic compressor.

| Time-averaged performance | Excitation | Designed condition | |
|---|---|---|---|
| | | $\Delta$ | $\delta/\%$ |
| $\pi$ | Symmetric | −0.0052 | −0.33 |
| | Asymmetric | −0.0077 | −0.49 |
| $\eta$ | Symmetric | −0.4 | −0.5 |
| | Asymmetric | 1.28 | 1.6 |
| $SM$ | Symmetric | 0.332 | 237.1 |
| | Asymmetric | 0.107 | 76.4 |

**Table 9** Experiment results on a low speed compressor at distorted inlet flow.

| Time-averaged performance | Excitation | Designed condition | |
|---|---|---|---|
| | | $\Delta$ | $\delta$/% |
| $\Delta P^*$ | Symmetric | −12.5 Pa | −0.8 |
| | Asymmetric | −0.4 Pa | 0.0 |
| $\eta$ | Symmetric | −0.7 | −0.86 |
| | Asymmetric | 0.7 | 0.86 |
| *SM* | Symmetric | 0.747 | 236.4 |
| | Asymmetric | 0.474 | 150 |

(3) In the current aero-thermodynamic design system, the whole flow-field of WS propulsion system is divided into several sub-systems, one of which is CS. However, there is no clear-cut boundary in the actual flow-field, and thus how to arrange the coupling between CS and its upstream and downstream sub-systems is another possible technical approach for facilitating the transformation from UNF into UCF.
(4) Low speed and high speed axes of WS engines are co-rotating or contra-rotating, which will exert strong influences on the unsteady flow-field, technical approaches facilitating the transformation from UNF into UCF under this condition and related schemes are still under exploration.

## Acknowledgments

The authors gratefully acknowledge the financial support received from the National Natural Science Foundation of China (Grant no. 10902008) for this project.

## References

[1] S. Zhou, Exploring on three new concepts of aero-thermodynamic in turbofan engine, Xiangshan Science Conference 176 "Major Infrastructure Issues on Airspace Security", Beijing, 2001 (in Chinese).
[2] R.C. Dean, On the necessity of unsteady flow in fluid mechanics, ASME Journal of Basic Fluids (1959) 24–28.
[3] A.P. Hou, Investigation on theory of two generations unsteady flow types in axial compressor, Dissertation, School of Energy and Power Engineering, Beihang University, Beijing, 2007 (in Chinese).
[4] J.Z. Wu, H.Y. Zhang, M.D. Zhou, Vortex Dynamic, High Education Press, Beijing, 1993 (in Chinese).
[5] H. Weimerskirch, J. Martin, Y. Clerquin, P. Alexandre, S. Jiraskova, Energy saving in flight formation, Nature 413 (2001) 685–686.
[6] Aero-Engine Design Manual Editorial Board, Aero-Engine Design Manual, No. 8: Compressor, Aviation Industry Press, Beijing, 2000 (in Chinese).
[7] I.A. Johnson, R.O. Bullock, Aerodynamic design of axial-flow compressor, Chapter 3,8,13, NASA SP-36, 1965.
[8] Z.Q. Gong, Measurement and comparative analysis of unsteady cooperative flow structures in an axial compressor, Dissertation, School of Energy and Power Engineering, Beihang University, Beijing, 2008 (in Chinese).
[9] X.Q. Zheng, Investigation on the conditions of flow pattern transform in unsteady vortex flow-field of axial compressors, Dissertation, School of Energy and Power Engineering, Beihang University, Beijing, 2005 (in Chinese).
[10] S. Zhou, X.Q. Zheng, A.P. Hou, Y.J. Lu, Interaction of unsteady separated flow over multi-bodies moving relatively in the same flow-field, Journal of Sound and Vibration 288 (4–5) (2005) 981–1009.
[11] B.G. Tong, B.X. Zhang, E.J. Cui, Unsteady Flow and Vortex Movement, National Defense Industry Press, Beijing, 1993 (in Chinese).
[12] S. Zhou, A.P. Hou, Y.J. Lu, Exploring on a forefront studying direction of aero-thermodynamic in turbo-machinery, in: Essays on the Forefront Studying of Aerodynamic, China Aerospace Press, Beijing, 2003 (in Chinese).
[13] J. Zhang, S. Zhou, L. Qing, A new model for describing inherent unsteady flow in turbo-machinery, International Journal of Turbo & Jet Engines 18 (4) (2001) 259–276.
[14] Z.P. Li, Experimental investigation of realizing unsteady cooperative flow type in axial-flow compressor, Dissertation, School of Energy and Power Engineering, Beihang University, Beijing, 2006 (in Chinese).
[15] Z.P. Li, Q.S. Li, W. Yuan, A.P. Hou, Y.J. Lu, Y.L. Wu, Experimental study on unsteady wake impacting effect in axial-flow compressors, Journal of Sound and Vibration 325 (1–2) (2009) 106–121.
[16] J.S. Xiong, Investigation on circumferential configuration in axial-flow compressor aerodynamic design, Dissertation, School of Energy and Power Engineering, Beihang University, Beijing, 2007 (in Chinese).
[17] X.B. Zhou, Investigation on the unsteady vortex sheet in unsteady vortex flow field of axial compressors, Dissertation, School of Energy and Power Engineering, Beihang University, Beijing, 2008 (in Chinese).
[18] W. Yuan, The research on the influence of casing treatment geometry on compressor characteristic, Dissertation, School of Energy and Power Engineering, Beihang University, Beijing, 2007 (in Chinese).
[19] X.Z. Song, Investigation on the maximal aerodynamic load of the integral transonic fan stage, Dissertation, School of Energy and Power Engineering, Beihang University, Beijing, 2008 (in Chinese).
[20] C.H. Yu, Investigation on methods for improving end-wall unsteady space-time flow field in axial flow compressors, Dissertation, School of Energy and Power Engineering, Beihang University, Beijing, 2008 (in Chinese).
[21] Y.J. Lu, Turbo-Machinery Unsteady Flow Theory, Beihang University Press, Beijing, 1990 (in Chinese).
[22] H.B. Jiang, Experimental investigation on the unsteady cooperative flow control for the compressor with inlet distortion, Dissertation, School of Energy and Power Engineering, Beihang University, Beijing, 2008 (in Chinese).
[23] Q.S. Li, Numerical simulation and experiment study for counter-rotating axial compressor, Dissertation, School of Energy and Power Engineering, Beihang University, Beijing, 2000 (in Chinese).
[24] J. Zhang, The research on blade row flow marching in multistage axial turbomachinery, Dissertation, School of

Energy and Power Engineering, Beihang University, Beijing, 2007 (in Chinese).
[25] S. Zhou, X.Q. Zheng, A.P. Hou, Y.J. Lu, Interaction of unsteady separated flow over multi-bodies moving relatively in the same flow-field, Journal of Sound & Vibration 288 (4–5) (2005) 981–1009.
[26] W. Tuo, Investigation of the influence of casing treatment on whole span flow field in a transonic compressor, Dissertation, School of Energy and Power Engineering, Beihang University, Beijing, 2009 (in Chinese).